

# Dynamic Model of Automatic Loom on SimulationX

A. Jomartov, A. Tuleshov, B. Tultaev

**Abstract**—One of the main tasks in the development of textile machinery is to increase the rapidity of automatic looms, and consequently, their productivity. With increasing automatic loom speeds, the dynamic loads on their separate mechanisms and moving joints sharply increase. Dynamic research allows us to determine the weakest mechanisms of the automatic loom. The modern automatic loom consists of a large number of structurally different mechanisms. These are cam, lever, gear, friction and combined cyclic mechanisms. The modern automatic loom contains various mechatronic devices: A device for the automatic removal of faulty weft, electromechanical drive warp yarns, electronic controllers, servos, etc. In the paper, we consider the multibody dynamic model of the automatic loom on the software complex SimulationX. SimulationX is multidisciplinary software for modeling complex physical and technical facilities and systems. The multibody dynamic model of the automatic loom allows consideration of: The transition processes, backlash at the joints and nodes, the force of resistance and electric motor performance.

**Keywords**—Automatic loom, dynamics, model, multibody, SimulationX.

## I. INTRODUCTION

**D**YNAMIC research of the machine starts with the development of a dynamic model in which we must take into account the most significant dynamic parameters. The dynamic model is an idealized image of the real machine. The dynamic model is used for theoretical and engineering research [1]-[4]. The real machine has an infinite number of degrees of freedom. Let's suppose that the inertial parameters of the machine parameters are concentrated at particular points. The points are connected without inertia and elastic-dissipation. Using these assumptions, we obtain a dynamic model with a limited number of degrees of freedom. Selecting a dynamic model of the machine depends on the initial information about the parameters of the machine mechanisms. To select a dynamic model of the machine is important carrying out of the experimental researches of the machine [5]-[7].

One important task of textile engineering is to increase automatic loom productivity. To increase loom productivity, it is necessary to increase the operating speeds of the drive machine. As a result of this, the dynamic loads of the units and mechanisms of the machine are increased [8], [9]. The research of automatic loom dynamics is now the current problem. The modern automatic loom is a complex mechanical system. In the process of forming fabric, a large number of different

mechanisms are involved. This are widespread cyclic mechanisms, dynamic models which can be presented in a more or less complex form depending on the goals and tasks of the research.

## II. AUTOMATIC LOOM

The automatic looms (see Fig. 1) with mini projectile are designed to produce wool, cotton, linen, silk and polypropylene fabrics filling widths of 180, 220, 250, 330 cm [9]. One of the main features of the automatic loom is the method of laying of weft into the shed. Instead of a shuttle for the insertion of the weft, these automatic looms use the steel plate of the tubular section as projectiles, with a spring mounted to capture and hold the weft yarn. The small size and the mass (6,35x14x90 mm, 40 g) of the projectiles can significantly improve the speed of the automatic looms. Fixed bobbins with the yarn are installed on the left side of the automatic loom. The number of bobbins is defined by the color of the weft and can reach up to 4. On the automatic loom, the insertion of weft thread into the shed is carried on the left side of the automatic loom. The projectile of weft is flying in the shed on the guide comb, consisting of separate metal plates. The empty projectiles of weft are returned to the weft-fighting box using the transporter. The beat-up mechanism of the automatic looms consists of the cams, which are located on the main shaft of the loom. The drive of the beat-up mechanism is located in the oil boxes. The swing of the beat-up mechanism is small, about 80 mm, and the blade is 7-9 times shorter than the conventional blades of a shuttle machine.

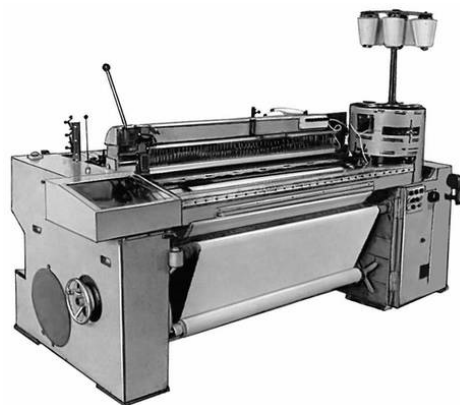


Fig. 1 The automatic loom

A. Jomartov is with the Institute Mechanics and Mechanical Engineering, Almaty, 050010, Kazakhstan, (corresponding author to provide phone: +7 777-329-5999, fax: +7 727-272-6270; e-mail: legsert@mail.ru).

A. Tuleshov is with the Institute Mechanics and Mechanical Engineering, Almaty, 050010, Kazakhstan, (e-mail: aman\_58@mail.ru).

B. Tultaev is with the Institute Mechanics and Mechanical Engineering, Almaty, 050010, Kazakhstan, (e-mail: b.tultaev@mail.ru).

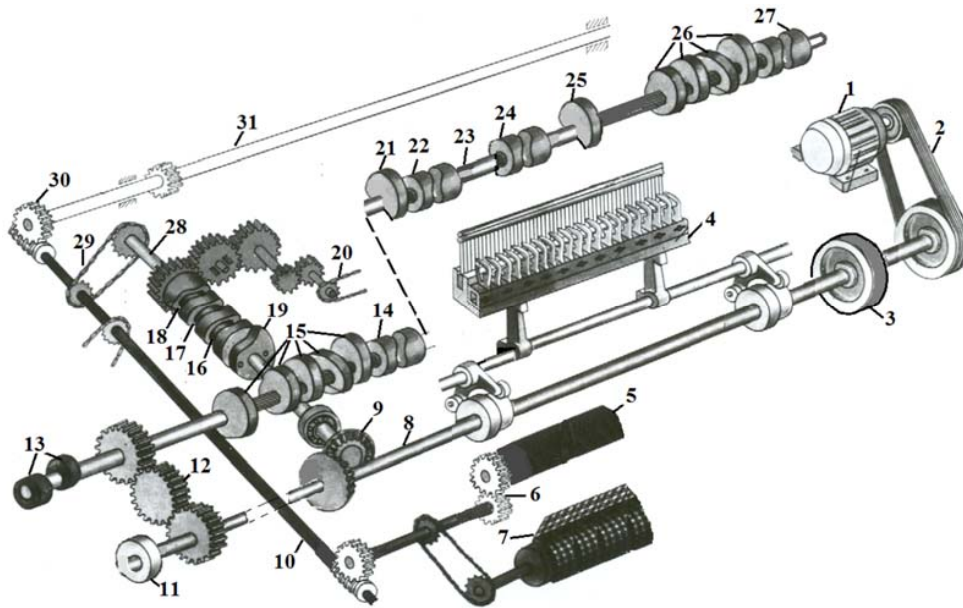


Fig. 2 The structural scheme of the automatic loom

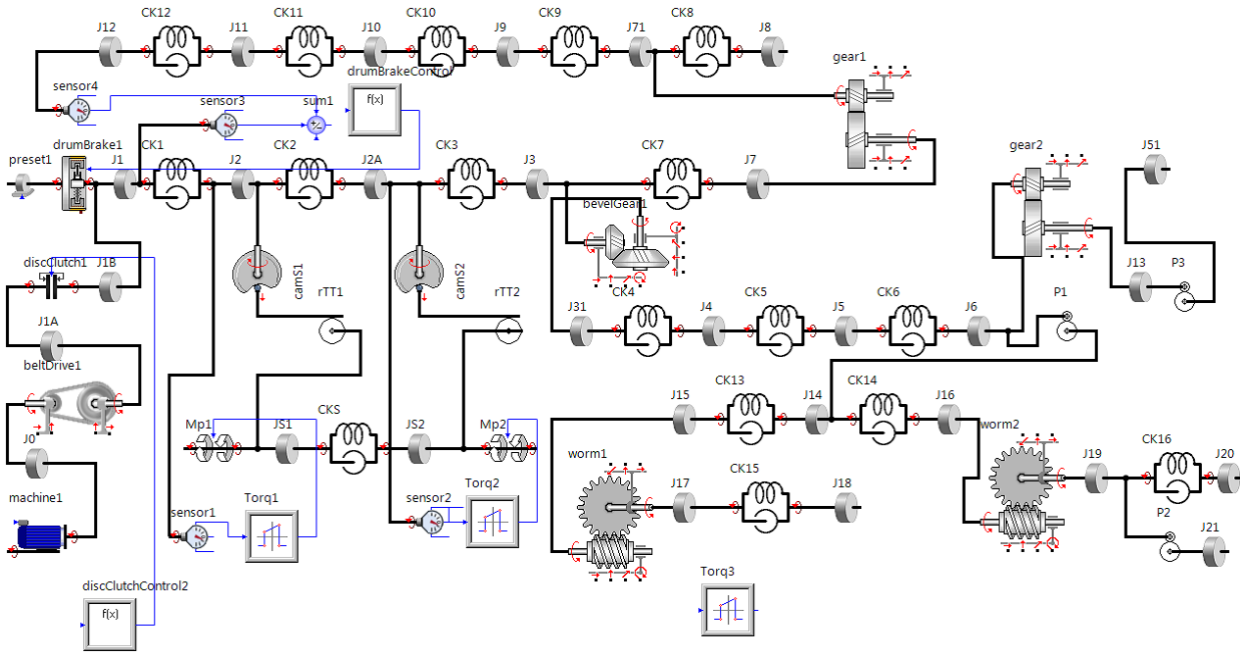


Fig. 3 The dynamic model of the automatic loom on SimulationX

The structural scheme of the automatic loom[9] is shown in Fig. 2, which shows the main units and mechanisms, where the following are denoted: 1 - the electric motor of the main drive shaft of the loom; 2 – the V-belt drive transmission of the main drive shaft of the loom; 3 - the brake; 4 - the beat-up mechanism; 5 – the breast beam; 6 - the drive of the breast beam; 7 - the cloth roll shaft; 8 - the main drive shaft of loom; 9 - the bevel gear; 10 - the lower shaft; 11 - the roller locking mechanism; 12 - the gear; 13 - the drive of mechanisms of the weft brake and the weft tension compensator; 14 - the drive of

the mechanism of the projectile feeder of the weft; 15 - the drive of mechanisms of the upper left box; 16,17,18,19 - the drives of the mechanisms of the left weft box: the opener of springs of the projectile of the weft, the lifter of the projectile of the weft, the opener of the springs of the thread catcher, and the picking mechanism, respectively; 20 - the conveyor of the projectiles of the weft; 21 - the drive of the mechanism of the left scissors; 22 - the drive of the mechanism of left selvage formation; 23 - the upper shaft; 24 - the drive of the mechanism of right selvage formation; 25 - the drive of the mechanism of the right

scissors; 26 - the drive of the mechanisms of the right receiving box; 27 - the drive of the mechanism for pushing the projectile of the weft; 28 - the cross shaft of the left weft box; 29 - the drive of the lower shaft; 30 - the worm gear; 31 - the warp beam.

### III. DYNAMIC MODEL OF AUTOMATIC LOOM ON SIMULATIONX

The dynamics of the automatic loom may be simulated on the software package SimulationX [10]. The dynamic model of the automatic loom on SimulationX is shown in Fig. 3.

The elements of the SimulationX library [10] which are used in the model of the automatic loom are shown in Fig. 4.

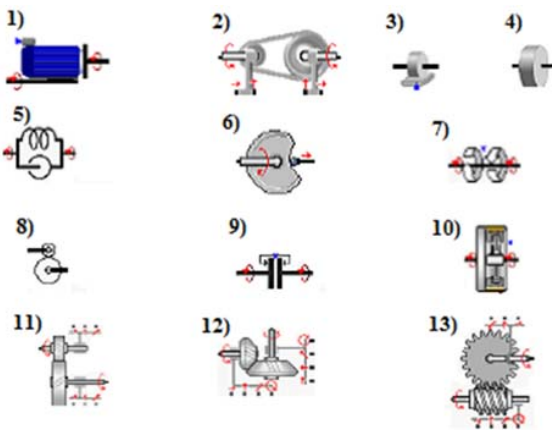


Fig. 4 The elements of the SimulationX library

Description of the elements of the SimulationX library (see Fig. 4.):

1. *Asynchronous Moto*: This element type models a simple asynchronous motor. The model is based on the steady-state characteristics of the motor. During start up, torques oscillating at the supply frequency of the power supply are superimposed on these characteristics. The model can be used even if only a few parameters are available to the user, and it represents the asynchronous motor with sufficient accuracy for many situations of drive train simulation. This includes switch-on and run-up processes, as well as the finding or setting of the operating point, dependent on load and/or rotational speed;
2. *Belt Drive*: The Belt Drive type models transmission behavior taking into consideration the belt elasticity and damping. The resulting bearing forces and displacements are provided at the mechanical bearing connectors in x and y direction for both wheels. This allows modeling of the interaction of the drive with its mounts as well as for instance preloads applied to the drive;
3. *Preset*: This element defines the angular displacement or the angular velocity or the angular acceleration;
4. *Inertia*: This element models the moment of inertia;
5. *Spring-Damper-Backlash*: This element models the elasticity, the dissipation and the backlash;
6. *Cam Disk Mechanism*: The model represents a rigid and ideal rotational-translational transformer. It models the transformation of torques and forces as well as the motion quantities between the rotational cam disk or groove profile body and the follower. The model does not consider rotational inertias or masses. Fields of application are models of cam disk and follower mechanisms (e.g., cam shaft drivetrains of combustion engines) or stepping gear mechanisms (e.g., in textile machines);
7. *External Torque*: This element type allows the injection of user-defined torques between two components or at one component only. It provides universal functionality for translating a signal quantity into a torque in the mechanical model. Thus, among other applications, it is well suited for the modeling of torque-deformation and torque-speed characteristics. Further, it can model static loads, for instance, and so on;
8. *Transmission*: This element models the transfer function of the mechanism;
9. *Disc Clutch*: The Disc Clutch model type represents a component which enables or interrupts a torque flow (and thus power transmission) between drive components. The model can be used for modeling multi-disk clutches of machines or gearboxes as well as classic automotive friction clutches. It is also possible to model friction brakes (e.g. of automatic transmission gearboxes). Depending on the clutch type, its actuation, and its parameter settings, the transition between the open and closed states can range from abrupt to smooth. The clutch considers stick and slip friction behavior as it is known from rigid or elastic friction elements. Clutch elasticity can be taken into account. By default, the element computes stiffness, damping, and friction parameters with catalog data. Options also allow the free definition of these parameters. In powertrain models, the clutch can be switched with a switch signal. Then, there is the approach of the rising pressure force up to its maximum (the maximum is a parameter) in a definable time range which is also parameter. It is also possible to shift the clutch by presetting the pressure force directly;
10. *Drum brake*: The drum brake model gathers a clutch between the drum and the environment as well as a thermal model for heating the drum. The model can be connected to a rotational system. This could be a vehicle wheel model for instance. The drum inertia is taken into account inside. At the stator side, a mounting structure can be connected. If nothing is connected at the stator side, the stator is fixed. If the mounting is modeled as elastic, an inertia element, representing the stator inertia (housing, feet, etc.) should be connected first;
11. *Gear*: The Gear stage model type can be used for the conversion of rotational speed and torque during the transmission process. It models the meshing of the gears, taking tooth stiffness and rotational backlash into account. It is suitable for modeling spur and helical gears. If required, the gear contact can be modeled as rigid. The radial and axial support behavior can be modeled

externally and thus can be rigid or elastic. Force, spring, and pre-load models are possible;

12. *Bevel gear*: The bevel gears model type can be used to change the direction of motion in a mechanical system by 90 degrees;
13. *Worm Gear*: This type models a Worm Gear transmission, considering the rotation of the worm and worm gear around their axes of rotation. Furthermore, translational and rotational connectors for support models are provided. The translational connectors give the possibility of representing translational degrees of freedom of the components. In some situations, it is also important to consider the inclination of the worm, e.g. axle bending.

The moments of inertia and the stiffness coefficients in the dynamic model of the automatic loom on SimulationX (see Fig. 3): J0 - the moment of inertia of the drive pulley; J1A, J1B - the moments of inertia of the driven pulleys; J1 - the moment of inertia of the brake of the main shaft; J2, J3 - the moments of inertia of the cams of the beat-up mechanism; J3, J31 - the moments of inertia of the bevel gear; J5 - the moment of inertia of the cam; J6, J7 - the moments of inertia of the gear; J71 - the moment of inertia of the cam; JS1, JS2 - the moments of inertia of the shaft of the beat-up mechanism; J13, J51 - the moments of inertia of the conveyor gears; J15, J16 - the moments of inertia of the worms gear; J17, J18 - the moments of inertia of the warp beam; J19, J20 - the moments of inertia of the breast beam; J21 - the moments of inertia of the cloth roll shaft; J4 - the variable reduced moment of inertia of the picking mechanism; J8 - the variable reduced moment of inertia of the weft brake and the weft tension compensator; J9 - the variable reduced moment of inertia of the left weft box: the projectile feeder mechanism of the weft, the left weft scissors, the centering device, the left weft controller; J10 - the variable reduced moment of inertia of the left selvedge forming mechanism and thread catcher; J11 - the variable reduced moment of inertia of the right selvedge forming mechanism and thread catcher; J12 - the variable reduced moment of inertia of the mechanisms for braking and returning the projectile, the mechanism for pushing the projectile of the weft, the right weft controller; J14 - the variable reduced moment of inertia of the following mechanisms: lifting of frames, shed forming and color changing of weft; CK1 ÷ CK16 – the stiffness coefficients of the shafts; CKS - the stiffness coefficients of the shaft of the beat-up mechanism.

#### IV. THE INITIAL PARAMETERS OF THE MODEL

The power of the electric motor of automatic loom is  $W = 1.7$  kW, and the engine speed is  $n = 1440$  rpm. The numerical values of the moments of the mechanisms of the automatic loom and the stiffness coefficients of the shafts are taken from [9]. *The dissipation coefficients* will be calculated by the following method: We consider the equivalent linearization of the dissipative forces in an oscillating system with many degrees of freedom. We presented that the dynamic model is quasi-linear, meaning that nonlinear dissipative forces have

negligible influence on the natural frequencies and mode shapes [2].

The system of differential equations of the model with  $H$  degrees of freedom is represented in the form:

$$\mathbf{a}\ddot{\mathbf{q}} + \mathbf{c}\dot{\mathbf{q}} = \mathbf{Q}, \quad (1)$$

where  $\mathbf{a}, \mathbf{c}$  are the square matrices of inertial and quasi-elastic coefficients;  $\mathbf{q}$  is the vector matrix (column) of the generalized coordinates;  $\mathbf{Q}$  is the vector matrix of non-conservative forces.

In the vector matrix of generalized forces, we distinguish the dissipative component of  $\mathbf{R}(\mathbf{q}, \dot{\mathbf{q}})$ , which is identified as

$$\mathbf{R} = -\mathbf{b}\dot{\mathbf{q}},$$

where  $\mathbf{b}$  is the square matrix of equivalent dissipative coefficients;  $\dot{\mathbf{q}}$  is the vector of generalized velocities.

We introduce the normal coordinates  $\theta_r, r = \overline{1, H}$

$$q_j = \sum_{r=1}^H \beta_{jr} \theta_r,$$

where  $\beta_{jr}$  - the coefficients of the form are defined without considering the dissipative forces. Then the system of differential equations (1) is represented as

$$\mathbf{a}^* \ddot{\boldsymbol{\theta}} + \mathbf{c}^* \dot{\boldsymbol{\theta}} = \mathbf{Q}^*, \quad (2)$$

where  $\mathbf{a}^* = \boldsymbol{\beta}^T \mathbf{a} \boldsymbol{\beta}$ ,  $\mathbf{c}^* = \boldsymbol{\beta}^T \mathbf{c} \boldsymbol{\beta}$ , are the diagonal matrices of inertial and quasi-elastic coefficients after the transition to the normal coordinates;  $\mathbf{q}, \mathbf{Q}^*$  are the vector matrices of the normal coordinates and the generalized non-conservative forces;  $\boldsymbol{\beta}$  is the coefficient matrix of forms. Next, we introduce to each of the equations of system (2) the equivalent dissipative force  $R_r = -b_r^* \dot{\theta}_r$ . Then

$$a_r^* \ddot{\theta}_r + b_r^* \dot{\theta}_r + c_r^* \theta_r = F_r^*(t),$$

where

$$F_r^* = \sum_{j=1}^H Q_j \beta_{jr}$$

The scattering coefficient  $\psi_r^*$  corresponding to the form  $r$  is defined as

$$\psi_r^* = \sum_{j=1}^H \psi_j c_j \beta_{jr}^2 / \sum_{j=1}^H \beta_{jr}^2.$$

From here  $r$  - th the coefficient dissipation is defined by [1], [2]:

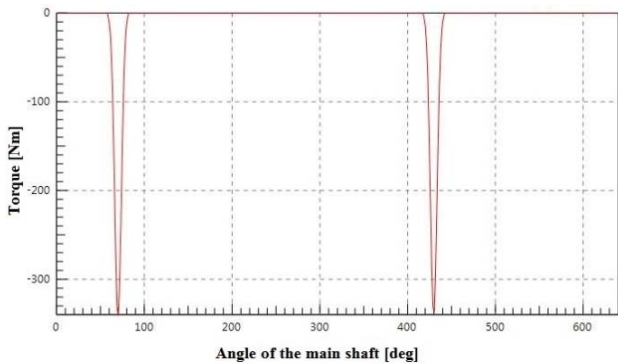
$$b_r^* = \frac{\psi_r^* c_r}{2\pi k_r}, \quad r = \overline{1, H},$$

where

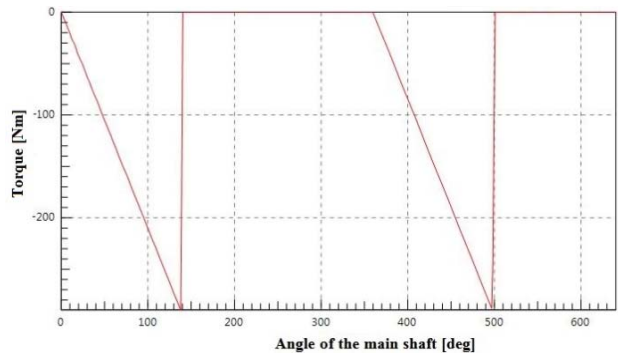
$$k_r = \sqrt{c_r / a_r}, \quad r = \overline{1, H},$$

$k_r$  - the natural frequencies of the system.

The resistance torques of the beat-up mechanism and the picking mechanism of the automatic loom are shown in Figs. 5 (a), (b).



(a)



(b)

Fig. 5 The resistance torques of the automatic loom: (a) the beat-up mechanism, (b) the picking mechanism

V. THE SIMULATION RESULTS

The calculation of a dynamic model of the automatic loom was carried out at an electric motor speed of 1440 rpm. Fig. 6 shows the natural frequencies of the automatic loom. Fig. 7 shows a Campbell diagram of the automatic loom.

As can be seen from the Campbell diagram (Fig. 7), the resonances arise for the 3rd harmonic of natural frequencies with revolutions of the main shaft of the automatic loom at  $n=380$  rpm and the 2nd harmonic of natural frequencies with revolutions of the main shaft of the automatic loom at  $n=560$  rpm. At present, the enterprises are developing a new high-speed automatic loom with the number of revolutions of the main shaft up to  $n=500$  rpm. It is therefore necessary take into account the second and third harmonics of the natural frequencies of the automatic loom in the design process.

Eigenvalues

No.	Value	f [Hz] (undamped)	f [Hz] (damped)	D [-]	Time Constant [s]
T1	-9.8947E-012				1.0106E+011
T2	8.7128E-005				-11477
T3	-34.741				0.028785
f1	-109.11+118.83 i	25.676	18.913	0.67634	0.0091647
f2	-109.11+118.83 i	25.676	18.913	0.67634	0.0091647
f3	-3.2286+275.23 i	43.808	43.805	0.01173	0.30973
f4	-3.2286+275.23 i	43.808	43.805	0.01173	0.30973
f5	-1.5809+316.2 i	50.326	50.325	0.0049996	0.63255
f6	-1.5809+316.2 i	50.326	50.325	0.0049996	0.63255
f7	-1.5808+316.2 i	50.326	50.325	0.0049993	0.63259
f8	-1.5808+316.2 i	50.326	50.325	0.0049993	0.63259
f9	-26.951+584.07 i	93.056	92.957	0.046094	0.037105
f10	-26.951+584.07 i	93.056	92.957	0.046094	0.037105
f11	-25.774+636.28 i	101.35	101.27	0.040474	0.038799
f12	-25.774+636.28 i	101.35	101.27	0.040474	0.038799
f13	-15.09+873.55 i	139.05	139.03	0.017272	0.066269
f14	-15.09+873.55 i	139.05	139.03	0.017272	0.066269
f15	-16.026+990.94 i	157.73	157.71	0.01617	0.0624
f16	-16.026+990.94 i	157.73	157.71	0.01617	0.0624
f17	-26.28+1245.9 i	198.34	198.3	0.021088	0.038052
f18	-26.28+1245.9 i	198.34	198.3	0.021088	0.038052
f19	-35.64+1483.7 i	236.2	236.13	0.024014	0.028059
f20	-35.64+1483.7 i	236.2	236.13	0.024014	0.028059
f21	-17.574+1576.2 i	250.88	250.87	0.011149	0.056902
f22	-17.574+1576.2 i	250.88	250.87	0.011149	0.056902
f23	-17.629+1578.7 i	251.27	251.26	0.011166	0.056726
f24	-17.629+1578.7 i	251.27	251.26	0.011166	0.056726
f25	-56.624+1891.5 i	301.18	301.05	0.029922	0.01766
f26	-56.624+1891.5 i	301.18	301.05	0.029922	0.01766
f27	-99.424+2505.6 i	399.1	398.78	0.039649	0.010058
f28	-99.424+2505.6 i	399.1	398.78	0.039649	0.010058
f29	-113.29+2674.4 i	426.02	425.64	0.042324	0.0088269
f30	-113.29+2674.4 i	426.02	425.64	0.042324	0.0088269
f31	-180.48+3373.7 i	537.71	536.94	0.053419	0.0055408
f32	-180.48+3373.7 i	537.71	536.94	0.053419	0.0055408
f33	-249.95+3968.1 i	632.8	631.54	0.062866	0.0040008
f34	-249.95+3968.1 i	632.8	631.54	0.062866	0.0040008
f35	-276.11+4169.7 i	665.08	663.63	0.066073	0.0036218
f36	-276.11+4169.7 i	665.08	663.63	0.066073	0.0036218

Fig. 6 The natural frequencies of the automatic loom

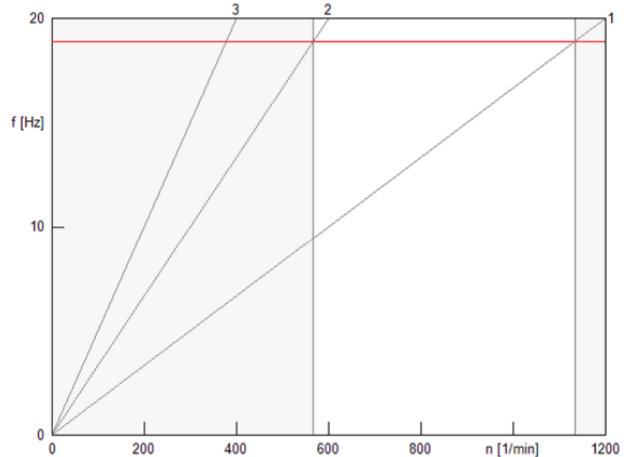
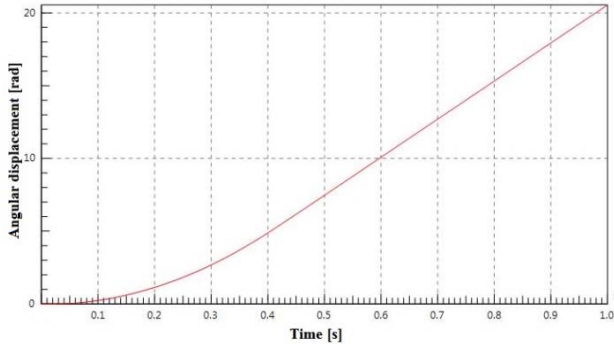


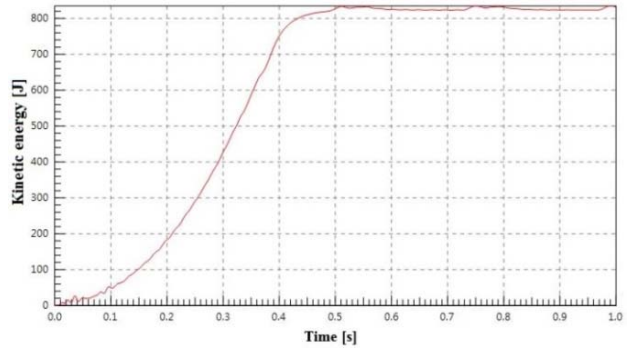
Fig. 7 A Campbell diagram of the automatic loom

The angular displacement, angular velocity and angular acceleration of the flywheel of the main shaft of the automatic loom are shown in Figs. 8 (a), (b) and (c), respectively.

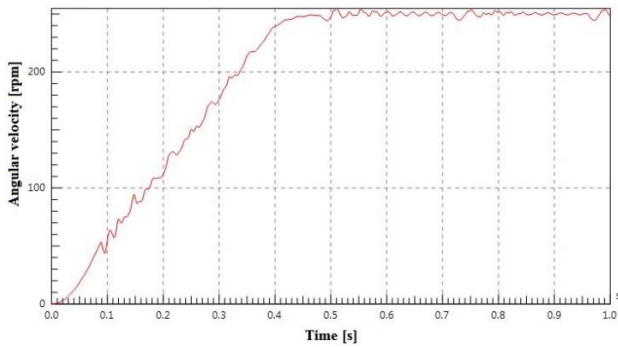
The input energy from the electric motor, kinetic energy, potential energy and dissipation energy of the automatic loom are shown in Figs. 9 (a), (b), (c) and (d), respectively.



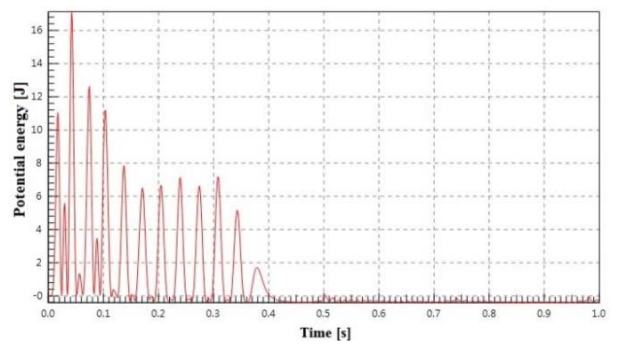
(a)



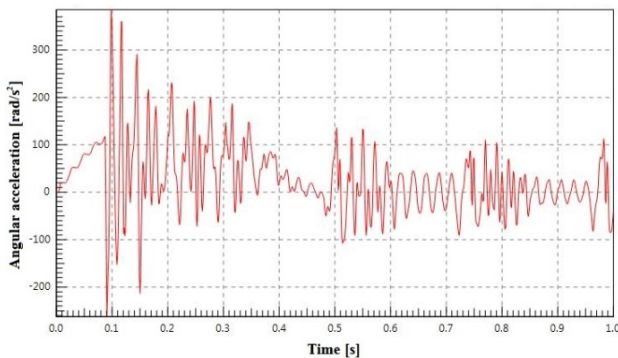
(b)



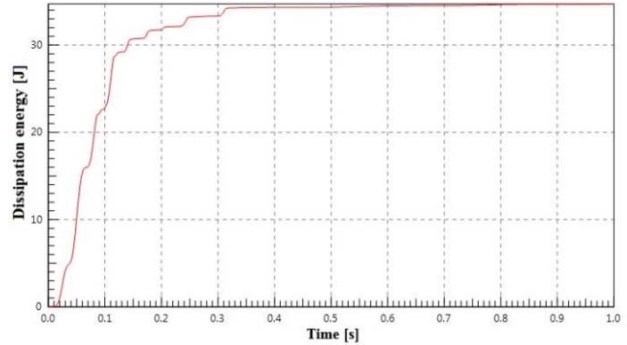
(b)



(c)



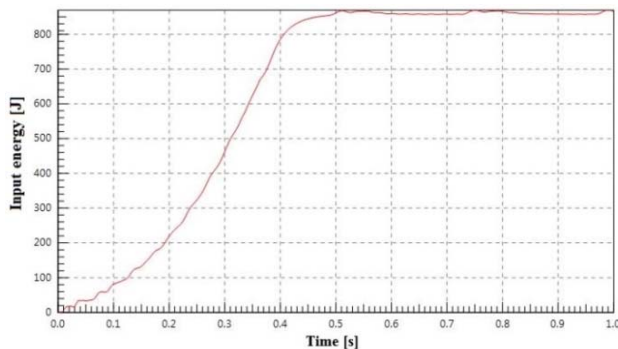
(c)



(d)

Fig. 8 The flywheel of the main shaft of the automatic loom: (a) Angular displacement, (b) Angular velocity, (c) Angular acceleration

Fig. 9 Energies of the automatic loom: (a) Input energy from the electric motor, (b) Kinetic energy, (c) Potential energy, (d) Dissipation energy



(a)

## VI. CONCLUSION

A dynamic model of the automatic loom on the software package SimulationX was developed. A dynamic model of the automatic loom on the software package SimulationX allows a consideration of the elastic and dissipative properties of the links of mechanisms, backlashes in the joints and components, resistance forces and the characteristics of the electrical motor. The natural frequencies of the automatic loom were determined. The influence of 2nd and 3rd harmonics on the resonance vibrations of the loom for the varying angular velocity of the main shaft of the loom was analyzed. The angular displacement, angular velocity and angular acceleration of the flywheel of the

main shaft, the drive of mechanisms of the right box, and the drive of mechanisms of the left box of the automatic loom were determined. The difference vibrations between the flywheel and the drive of mechanisms of the left and right boxes of the automatic loom were determined to estimate the influence of elastic and dissipative characteristics on the dynamics of the loom. An energy analysis of the automatic loom was determined. The input energy from the electric motor, kinetic energy, potential energy, and dissipation energy of the automatic loom were determined.

## REFERENCES

- [1] H. Dresig, F. Holzweißig, *Dynamics of Machinery*. Berlin: Springer, 2010.
- [2] H. Dresig, I.I. Vulfson, *Dynamik der Mechanismen*. Wien, New York: Springer-Verlag, 1989.
- [3] I. I. Vulfson, *Dynamics of cyclic machines*. Heidelberg, New York, London: Springer, 2015.
- [4] A. A. Shabana, *Dynamic of Multibody Systems*. Cambridge University Press, 2013
- [5] H. A.Youssef, H. El-Hofy, *Machining technology: machine tools and operations*. Taylor & Francis Group LLC., 2008.
- [6] M. Z. Kolovsky, A. N. Evgrafov, Yu.A. Semenov and A.V. Slousch, *Advanced theory of mechanisms and machines*. Berlin Heidelberg: Springer. 2000.
- [7] V. K. Astashev, V. I. Babitsky and M. Z. Kolovsky, *Dynamics and control of machines*. Berlin Heidelberg: Springer, 2000.
- [8] A. Jomartov, S. Joldasbekov and Yu. Drakunov, "Dynamic synthesis of machine with slider-crank mechanism," *Mech. Sci.*, vol. 6, pp. 35-40, 2015.
- [9] A. A. Jomartov, G. Ualiyev, *The dynamics of the mechanisms of automatic looms STB*. Tauari, Almaty, 2003.
- [10] *Manual SimulationX 3.5*. Dresden: ITI GmbH ITI, in <http://www.simulationx.com/>. Accessed on 2/11/2016.